Thessaloniki-GREECE 2007

4th International Conference on
Earthquake Geotechnical Engineering
June 25-28, 2007
Paper No. 1382

A UNIFIED PREDICTION FOR LIQUEFACTION AND SETTLEMENT OF SATURATED SANDY GROUND

Ryosuke UZUOKA[1], Yuko SHIMIZU[2], Akiyoshi KAMURA, Noriaki SENTO[3], Motoki KAZAMA[4]

ABSTRACT

A unified prediction model for liquefaction and settlement of saturated sandy ground based on the minimum effective stress concept is proposed. Minimum effective stress can be easily applied to existing constitutive models proposed for liquefaction analyses. Performance of the new prediction method was verified through numerical simulations, based on the dynamic soil-water coupled theory, on laboratory tests as well as the dynamic centrifuge tests. Both liquefaction process during the excitation and consequent ground settlement during the excess pore water pressure dissipation process were well reproduced with the simulations.

Keywords: liquefaction, settlement, volumetric strain, elasto-plastic model, dynamic soil-water coupled analysis

INTRODUCTION

Although the settlement of liquefied ground has caused serious damages of structures (e.g. Ishihara 1993, Jefferies and Been 2006), a unified prediction for the occurrence of liquefaction and accompanying settlement of saturated sandy ground has not been achieved. Liquefaction analysis has been developed since 1980’s by many researchers. The field equations of these liquefaction analyses are mainly based on Biot’s porous media theory (1962). Although several formulations, which use different unknown variables, for example, u-U, u-w and u-p formulations, have been used, their differences are not significant in the earthquake applications (Zienkiewicz and Shiomi, 1984). The performance of constitutive models, on the other hand, affects analytical results considerably, because the applicability of current constitutive models has not yet been sufficiently confirmed (Arulanandan and Scott, 1994). Further validation and modification of constitutive models in liquefaction analyses are necessary through simulations of laboratory tests, model experiments and case histories.

The volumetric compression of sand after liquefaction has been investigated with laboratory tests including undrained shear process and consequent drained compression process with dissipation of excess pore water pressure after liquefaction. It is reported that volumetric strain characteristics after liquefaction depends on the experienced strain histories (e.g. Lee and Albaisa 1974, Nagase and Ishihara 1988, Sento et al. 2004). Recent research (Sento et al. 2004) pointed out that liquefied sand experienced large strain histories yields large volumetric strain change during the dissipation of excess pore water pressure. Although some simplified evaluation methods of settlement of liquefied ground have been proposed (e.g. Tokimatsu and Seed 1987, Ishihara and Yoshimine 1992), most liquefaction analyses mainly focused on the liquefaction process and the shear deformation of the ground. Few

[1] Associate Professor, Department of Civil Engineering, Tohoku University, Japan, Email: uzuoka@civil.tohoku.ac.jp
[2] Graduate Student, Department of Civil Engineering, Tohoku University, Japan
[3] Research Associate, Department of Civil Engineering, Tohoku University, Japan
[4] Professor, Department of Civil Engineering, Tohoku University, Japan

analyses qualitatively discussed the settlement of liquefied ground after the dissipation of excess pore water pressure (Yoshida and Finn 2000). This study proposes a unified prediction model for liquefaction and settlement of saturated sandy ground based on the concept of minimum effective stress. Utilizing the dynamic soil-water coupled analysis with the proposed model numerical simulations are performed on dynamic centrifugal model tests, and find the proposed method can reproduce a unified behavior of saturated sandy ground during and after liquefaction

CONCEPT OF MINIMUM EFFECTIVE STRESS

A concept of minimum effective stress is introduced in order that the constitutive model can quantitatively reproduce the amount of volumetric strain with the dissipation of excess pore water pressure after liquefaction. Here we assume a simplified condition as shown in Figure 1 in which isotropically consolidated sand is subjected to undrained cyclic shear and the excess pore water pressure dissipates after liquefaction as shown in Figure 1. From the view point of the elasto-plastic theory, the increment of volumetric strain can be expressed as follows:

$$dv = dv^E + dv^P = \frac{\kappa}{(1+e)\sigma'_m} d\sigma'_m + Dd\gamma^P \tag{1}$$

where dv is the volumetric strain increment, dv^E is the elastic volumetric strain increment, dv^P is the plastic volumetric strain increment, κ is the swelling index, e is the initial void ratio, $d\sigma'_m$ is the mean effective stress increment, D is the dilatancy coefficient and $d\gamma^P$ is the second invariant of incremental deviatoric strain tensor. The dissipation process of the excess pore water pressure after liquefaction can be assumed as an elastic process because no plastic volumetric strain changes in the overconsolidation region without shear deformation. By neglecting plastic volumetric components, we can use the elastic linear relationship between the logarithms of mean effective stress and void ratio as shown by the broken line shown in Figure 1. In addition, the minimum effective stress σ'_{ml} as follows is defined as the intersection between the undrained path and dissipation path shown in Figure 1:

$$\sigma'_m \geq \sigma'_{ml} = R_{\lim}\sigma'_{m0} \tag{2}$$

where $R_{\lim}$ is the ratio of σ'_{ml} for the initial mean effective stress σ'_{m0} (parameter of liquefaction intensity). The typical measured path during the dissipation process is also shown in Figure 1. The measured minimum effective stress does not always coincide with the theoretical minimum effective stress σ'_{ml} due to the limit of measurement.

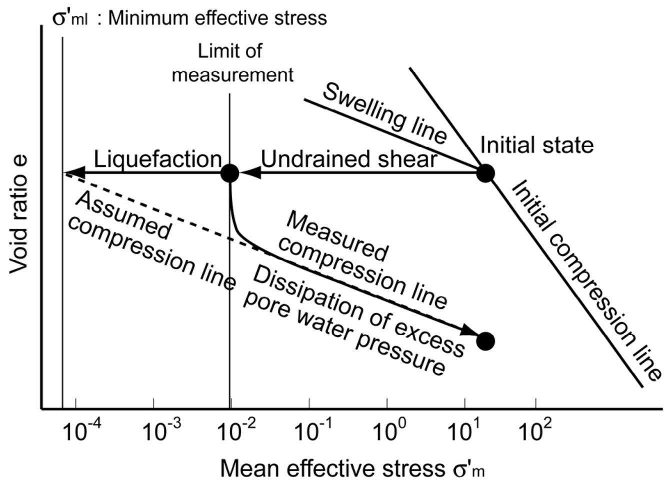

Figure 1. Concept of minimum effective stress

Sento et al. (2004) measured the volumetric strain of liquefied sand after dissipation of excess pore water pressure with torsional shear tests under various shear strain histories, and reported the limit of measurement for small mean effective stress at a liquefied state as shown in Figure 1. Thereby, they changed σ'_{ml} with the density of sand and strain history as follows:

$$R_{\lim} = 10^{-x} \quad x = \frac{a\gamma^P}{1+\gamma^P / b} \tag{3}$$

where a and b are the material parameters. Sento et al. (2004) reproduced the volumetric strain of liquefied sand after dissipation of excess pore water pressure using the elastic component of equation (1) and equation (2) and (3). Figure 2 (a) shows the measured and computed relationships between mean effective stress and volumetric strain during the dissipation of excess pore water pressure after liquefaction for different liquefaction intensities defined in equation (2) for medium dense Toyoura sand. Toyoura sand is fine uniform sand with a mean diameter D_{50} of 0.16 mm and a uniformity coefficient U_c of 1.2. The computed relationships agree with the experimental relationships for different liquefaction intensities. Figure 2 (b) shows the relationships between $R_{\lim}$ used in the computed relations in Figure 2 (a) and accumulated shear strain. The accumulated shear strain means the summation of the second invariant of incremental deviatoric strain from the initial state. The small $R_{\lim}$ implies a high intensity of liquefaction caused by large accumulated shear strain.

Utilizing the equations (1) - (3), we can calculate the elastic volumetric strain in the framework of the elasto-plastic model. Although the minimum effective stress can be related to the plastic volumetric strain during shear deformation, this simplified method is easy to be applied to practical problems. The minimum effective stress σ'_{ml} is also the lower bounds of the mean effective stress to keep numerical stability. It is noted that the σ'_{ml} has physical meaning previously discussed as equation (2) in this study, although it has been treated as a numerical parameter in past liquefaction analyses.

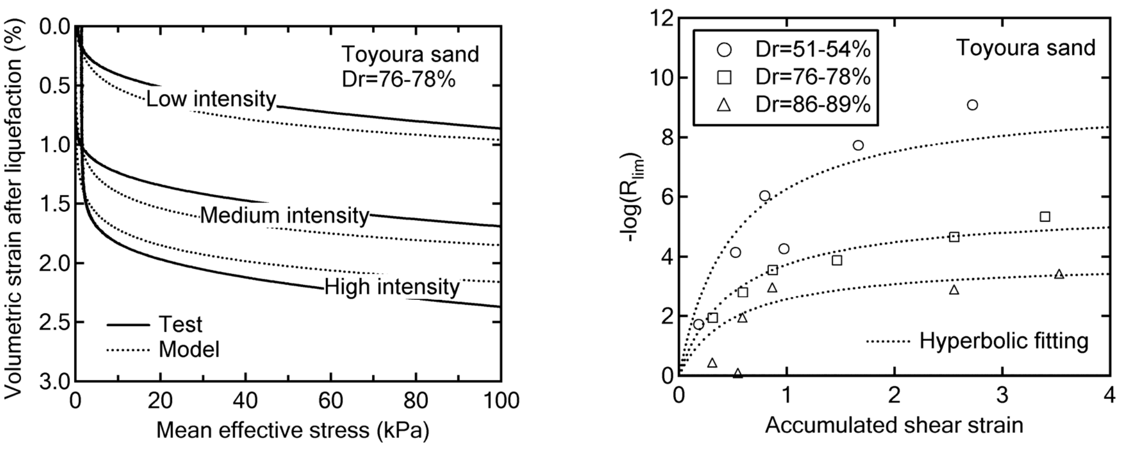

(a) volumetric strain after liquefaction (b) parameter of liquefaction intensity $R_{\lim}$

Figure 2. Parameter of minimum effective stress

VALIDATION OF THE PROPOSED CONSTITUTIVE MODEL

Modification of existing constitutive model

By adopting the minimum effective stress concept, an existing elasto-plastic constituting model (Oka et al. 1999) is modified. The existing constitutive equation is formulated based on the following concepts; 1) the elasto-plastic theory, 2) the non-associated flow rule, 3) the concept of the overconsolidated boundary surface, 4) the non-linear kinematic hardening rule and 5) the plastic strain-dependent plastic and elastic modulus. Oka et al. (1999) applied the constitutive model to the cyclic undrained behavior of sand through the numerical simulation of hollow cylindrical shear tests, and showed that the simulation reproduced experimental results well under various stress conditions, such as isotropic and anisotropic consolidated conditions, with and without the initial shear stress conditions, principal stress axis rotation, etc.

The modification of the existing constitutive model is easy if the constitutive model is based on the same assumption as equation (1). Although Oka's constitutive model assumes the equation (1), the swelling index (or elastic bulk modulus) is dependent on plastic strain history. Hence the swelling index is modified to be constant in this study.

Laboratory tests

Undrained and drained torsional shear tests were performed with careful evaluation of mean effective stress of the specimen. The specimen of the hollow cylindrical torsional shear test was 100 mm in outer diameter, 60 mm in inner diameter, and 100 mm in height. We used Toyoura sand as a testing material, which is the same material as that used in the dynamic centrifugal tests as mentioned later. Specimens were prepared by the air pluviated procedure and the relative density of about 40%, 65% and 80% at the end of the consolidation. The test samples were isotropically consolidated, the initial effective stress was 100 kPa with a backpressure of 200 kPa, and the B value was maintained at more than 0.95. The cyclic shear strain was applied under undrained condition in uniform triangular cycles with a constant strain rate. The shear strain amplitude increased from 0.1% (5 cycles), 0.2% (5 cycles), 0.5% (3 cycles), 1.0% (3 cycles), 2.0% (3 cycles) to 5.0% (1 cycle) in 6 stages. After undrained shear process, the liquefied specimen was isotropically reconsolidated with the drainage rate of 0.04%/min until the mean effective stress recovered the initial value. The responses of shear stress and pore water pressure were recorded. The recorded shear stress was corrected with a membrane tensile stress. The volumetric strain was also corrected with a membrane penetration effect (Vaid and Negussey 1984, Tokimatsu and Nakamura 1986, Goto 1986). The mean effective stress was calculated from vertical and lateral effective stress. The lateral effective stress was the measured differential pressure between inside the specimen and the outer cell pressure. The vertical effective stress was the sum of axial effective pressure and the self-weight of the specimen at the middle in height.

Table 1. Material parameters

Name of soil profile		Toyoura sand Dr=40%	Toyoura sand Dr=65%	Toyoura sand Dr=80%
Density	ρ (t/m^3)	1.91	-	-
Coefficient of permeability	k (cm/s)	0.0065	-	-
Initial void ratio	e_0	0.829	0.726	0.656
Compression index	λ	0.0045	0.0036	0.0031
Swelling index	κ	0.0032	0.0030	0.0026
Quasi-overconsolidation ratio	OCR^*	1.0	1.0	1.0
Failure stress ratio	M^*_f	1.097	1.170	1.290
Phase transformation stress ratio	M^*_m	0.714	0.714	0.714
Initial shear modulus ratio	G_0/σ'_m	354	436	555
Dilatancy parameter	D^*_0	1.5	1.0	1.0
	n	0.0	0.0	0.0
Hardening parameter	B^*_0	1100	1500	1800
	B^*_1	30	100	94
	C_f	500	1100	2000
Reference strain parameter	γ^{P*}_r	0.01	0.001	0.001
	γ^{E*}_r	0.01	0.05	0.1
R_{lim} parameter	a	24.0	15.0	8.6
	b	0.5	0.5	0.5

Determination of the material parameters

Model parameters of Toyoura sand with various relative densities are summarized in Table 1. Detailed description about the parameters can be referred to corresponding references (Oka et al., 1999). The following parameters, e_0, λ, κ, OCR^*, M_m^*, M_f^* and G_0/σ_m' were directly determined by physical property tests, isotropic consolidation process and undrained shear process. The parameters of $R_{\lim}$ were determined based on the results of volume compression tests (Sento et al. 2004). Although, in principle, remaining parameters could be determined by physical property tests and undrained monotonic and cyclic shear tests, the data adjusting method is more practical to determine the soil parameters. The values of material parameters were calibrated in order to provide a good description of the stress-strain relations and effective stress paths during undrained shear process.

Simulation of laboratory tests

The undrained shear and reconsolidation processes were simulated with the proposed constitutive model. The simulations of undrained shear and reconsolidation processes were performed with controlling the shear strain and the volumetric strain respectively. The increment of the strain was determined sufficiently small to keep the numerical accuracy. Figure 3 shows the measured and computed results of undrained shear process for the relative density of about 65%. The shear strain histories (a) were imposed to the specimen, and the shear stress and effective mean stress were computed. The constitutive model with calibrated material parameters can reproduce the test results very well.

Figure 4 shows the measured and computed results of drained reconsolidation processes for the relative density of about 40% and 65%. The constitutive model with calibrated material parameters can reproduce the final volumetric strain qualitatively and quantitatively. The measured mean effective stress less than about 0.5 kPa contains some measurement errors due to the electrical noise during the measurement. Although the compression curve is assumed to be linear in the constitutive model, the measured compression curves show some negative curvatures. This results show that the volumetric compression behavior of sand is not elastic even in overconsolidation region; therefore further investigation on modeling of volumetric compression behavior is necessary.

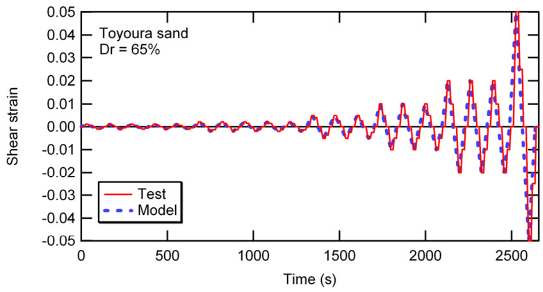

(a) shear strain histories

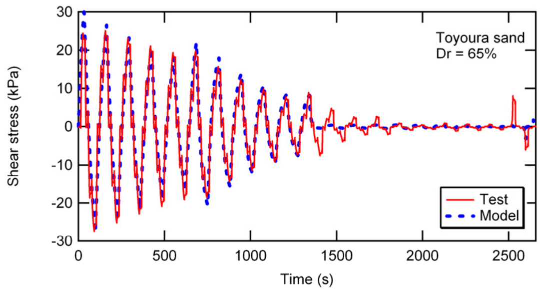

(b) shear stress histories

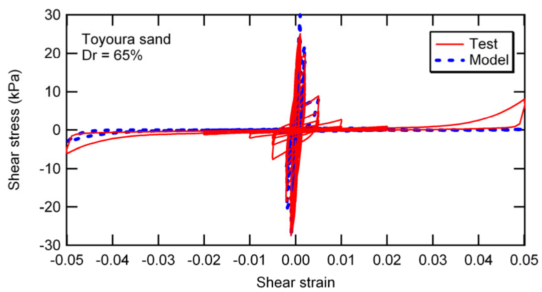

(c) stress – strain relations

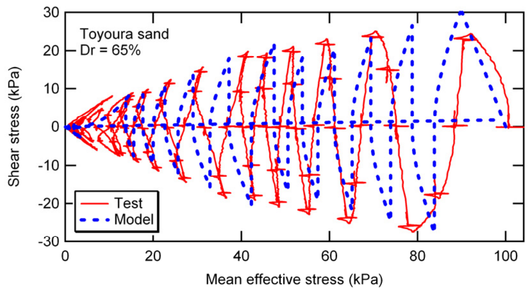

(d) effective stress paths

Figure 3. Measured and computed results of undrained shear process (Dr = 65%)

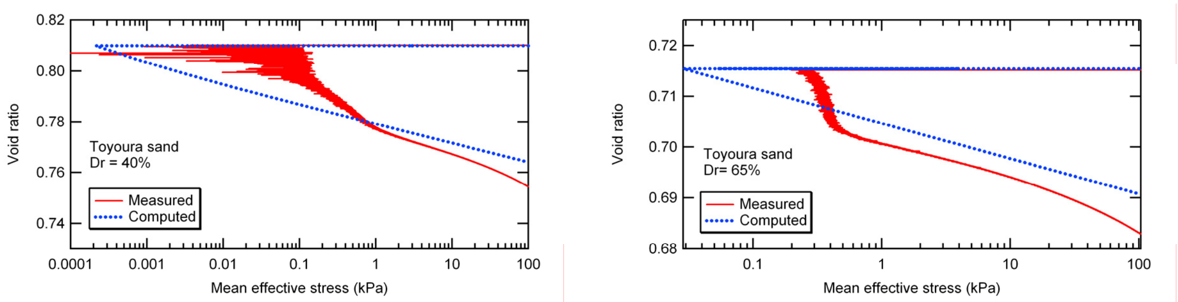

(a) Dr = 40% (b) Dr = 65%

Figure 4. Measured and computed results of drained reconsolidation process (Dr = 40 and 65%)

SIMULATION OF LIQUEFACTION-INDUCED SETTLEMENT

Numerical method

The numerical method is briefly described in this section. A dynamic soil-water coupled problem is formulated based on a u-p formulation (Oka et al., 1994). The finite element method (FEM) is used for the spatial discretization of the equilibrium equation, while the finite difference method (FDM) is used for the spatial discretization of the pore water pressure in the continuity equation. Oka et al. (1994) verified the accuracy of the proposed numerical method through a comparison of numerical results and analytical solutions for transient response of saturated porous solids. The governing equations are formulated basing on the following assumptions; 1) the infinitesimal strain, 2) the smooth distribution of porosity in the soil, 3) the small relative acceleration of the fluid phase to that of the solid phase compared with the acceleration of the solid phase, 4) incompressible grain particles in the soil. The equilibrium equation for the mixture is derived as follows:

$$\rho \ddot{\mathbf{u}}^S - \mathrm{div}\boldsymbol{\sigma} - \rho \mathbf{b} = \mathbf{0} \tag{4}$$

where ρ is the overall density, $\ddot{\mathbf{u}}^S$ is the acceleration vector of the solid, $\boldsymbol{\sigma}$ is the total stress tensor and $\mathbf{b}$ is the body force vector. The continuity equation is derived as follows:

$$\frac{n}{K^F}\dot{p} + \dot{\varepsilon}_v^S + \mathrm{div}\left\{\frac{k}{\gamma_w}\left(-\mathrm{grad}\, p + \rho^F \mathbf{b} - \rho^F \ddot{\mathbf{u}}^S\right)\right\} = 0 \tag{5}$$

where n is porosity, K^F is the bulk modulus of the fluid, p is the pore water pressure, $\dot{\varepsilon}_v^S$ is the volumetric strain rate of the solid, k is the coefficient of permeability, γ_w is the unit weight of the fluid, and ρ^F is the real density of the fluid. Newmark implicit method was used for time integration.

Dynamic centrifugal tests

The dynamic centrifugal tests were carried out with a circular laminar box under the 50 times gravity acceleration (Kawasaki et al. 1998). The horizontal model ground was made of homogeneous saturated Toyoura sand with the relative density of about 40%. The thickness of the model ground was 17.5m in prototype scale. The ground water level was set at the ground surface. The pore fluid was silicon oil with 50 times viscosity of water. The input acceleration at the table was a sinusoidal wave with the frequency of 1 Hz and the number of cycles of 20 in prototype scale. The amplitudes of acceleration were about 60 Gal in Case 1 and 90 Gal in Case 2 respectively. The measurements of pore water pressure, ground acceleration and settlement at the ground surface were made during and after the shaking.

Numerical data

A one-dimensional soil column model for the model ground was used for the simulation. The soil column comprised 35 isoparametric 4-noded solid elements. Only the ground water table at the surface was set to be permeable and the other boundaries were impermeable. The horizontal and vertical displacements at two nodes with the same depth were tied to reproduce free-field motion. The bottom of the soil column where the shaking motions were input is set to be rigid. The initial stress components for all elements were calculated by assuming the lateral earth pressure coefficient of 0.5. The proposed constitutive model was applied to all elements. The material parameters of Toyoura sand with the relative density of 40% were used in the simulation because the same material was used in the centrifugal tests.

A time integration step of 0.001 second was adopted to ensure the numerical stability. The hysteresis damping by the constitutive model was basically used, and Rayleigh damping proportional to initial stiffness was used in order to describe the damping especially in the high frequency domain. The factor of Rayleigh damping which was proportional to the initial ground stiffness was set to be 0.0025. The parameters in Newmark method were set to be 0.3025 and 0.6 to ensure the numerical stability.

Numerical results

Figure 5 and Figure 6 show the time histories of computed pore water pressures and ground accelerations respectively in both cases. The excess pore water pressures are picked up at the depth of 5 m and 10 m. The computed results with the original constitutive model also are shown in both figures. The complete liquefaction can be confirmed at about 3 seconds when the excess pore water pressure attains the initial effective overburden pressure and the ground acceleration becomes small. It is noted that both original and modified model show similar results before complete liquefaction; therefore it is easy to apply the proposed method to existing constitutive model. The discrepancy between the original and modified model is shown during the dissipation of excess pore water pressure. The dissipation with original model is much slower than that with modified model. This discrepancy will be discussed later.

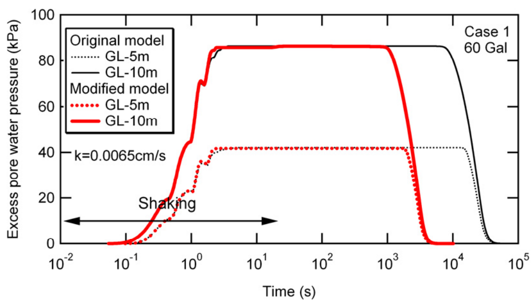

(a) Case 1 (60 Gal)

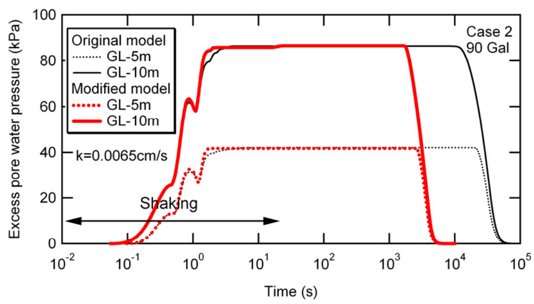

(b) Case 2 (90 Gal)

Figure 5. Computed time histories of excess pore water pressures

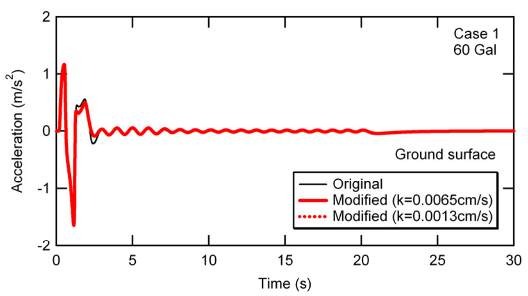

(a) Case 1 (60 Gal)

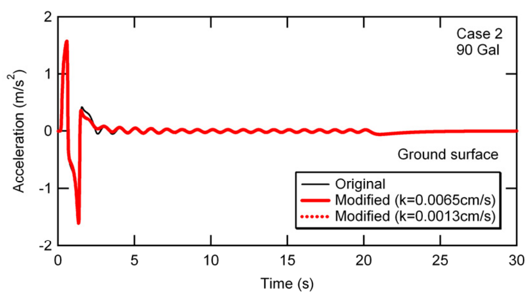

(b) Case 2 (90 Gal)

Figure 6. Computed time histories of ground accelerations

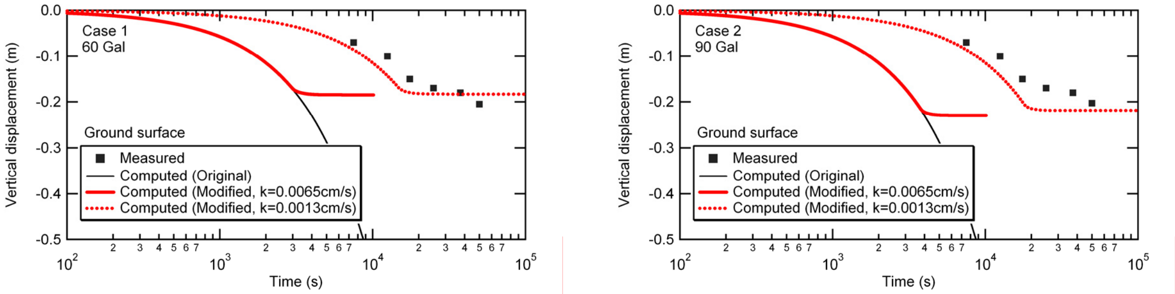

(a) Case 1 (60 Gal) (b) Case 2 (90 Gal)

Figure 7. Computed and measured time histories of ground settlements

Figure 7 shows the time histories of computed and measured ground settlements in both cases. The settlements with original model largely overestimate the measured ones because the material parameters of original model were calibrated only for the undrained shear process without the minimum effective stress concept. This overestimation of volumetric compression causes the delay in the dissipation of excess pore water pressure. The final settlements with modified model agree with the measured ones; however the convergence of settlement is earlier than the measurement in the case with the initial permeability of 0.0065 cm/s. The parametric cases with the permeability of 0.0013 cm/s are also shown in Figure 6 and 7. The results with the permeability of 0.0013 cm/s agree with the measurements. Although the decrease in permeability of liquefied ground is reasonable due to decrease in the void ratio, we need further investigation on the permeability of liquefied sand.

CONCLUSIONS

A unified prediction model for liquefaction and settlement of saturated sandy ground based on minimum effective stress concept is proposed. Minimum effective stress concept can be easily applied to existing constitutive models proposed for liquefaction analyses. The modified constitutive model was validated based on the results of undrained shear and consequent drained compression tests. The constitutive model with calibrated material parameters can quantitatively reproduce the final volumetric strain after liquefaction. Dynamic centrifugal model tests with saturated sandy ground were simulated with the dynamic soil-water coupled analysis incorporating the proposed model. The simulations reproduced the occurrence of liquefaction during the shaking process and consequent ground settlement during the dissipation process of excess pore water pressure. The computed ground settlements with the modified permeability quantitatively agree with the measured ground settlements.

ACKNOWLEDGEMENTS

The support of Special Project for Earthquake Disaster Mitigation in Urban Areas by Ministry of Education, Culture, Sports, Science and Technology is gratefully acknowledged. The authors wish to thank the research group chaired by Professor Tadanobu Sato, Waseda University and Professor Susumu Iai, Kyoto University. The authors thank Dr. Kenichi Horikoshi and Dr. Tadafumi Fujiwara, Taisei Corporation for their providing information about the centrifuge tests.

REFERENCES

Arulanandan K and Scott RF (ed.). Verification of Numerical Procedures for the Analysis of Soil Liquefaction Problems, Vol. 2, Balkema, Rotterdam, 1994.

Biot MA. “Mechanics of deformation and acoustic propagation in porous media,” J. Applied Physics, 33, 1482-1492, 1962.

Goto S. Strength and characteristics of granular materials in triaxial tests, Doctoral Thesis, University of Tokyo, 1986 (in Japanese).
Ishihara K and Yoshimine M. “Evaluation of settlements in sand deposits following earthquakes,” Soils and Foundations, 32, 1, 173-188, 1992.
Ishihara, K. “Liquefaction and flow failure during earthquakes,” Geotechnique, 43, 3, 351-415, 1993.
Jefferies M and Been K. “Soil liquefaction, a critical state approach,” Taylor and Francis, Oxford, 2006.
Kawasaki K, Sakai T, Yasuda S and Satoh M. “Earthquake-induced settlement of an isolated footing for power transmission tower,” Proc. Centrifuge 98, Tokyo, 271-276, 1998.
Lee KL and Albaisa A. “Earthquake induced settlements in saturated sands,” Journal of the Geotechnical Engineering Division, ASCE, 100, GT4, 387-406, 1974.
Nagase H and Ishihara K. “Liquefaction-induced compaction and settlement of sand during earthquakes,” Soils and Foundations, 28, 1, 65-76, 1988.
Oka F, Yashima A, Shibata T, Kato M and Uzuoka R. “FEM-FDM coupled liquefaction analysis of a porous soil using an elasto-plastic model,” Applied Scientific Research, 52, 209-245, 1994.
Oka F, Yashima A, Tateishi A, Taguchi Y and Yamashita S. “A cyclic elasto-plastic constitutive model for sand considering a plastic-strain dependence of the shear modulus”, Geotechnique, 49: 661-680, 1999.
Sento N, Kazama M and Uzuoka R. “Experiment and idealization of the volumetric compression characteristics of clean sand after undrained cyclic shear,” J. Geotechnical Engineering, JSCE, 764/III-67, 307-317, 2004 (in Japanese).
Tokimatsu K and Nakamura K. “A liquefaction test without membrane penetration effects, Soils and Foundations,” 26, 4, 127-138, 1986.
Tokimatsu K and Seed HB. “Evaluation of settlements in sands due to earthquake shaking,” Journal of Geotechnical Engineering, ASCE, 113, 8, 861-878, 1987.
Vaid YP and Negussey D. “A critical assessment of membrane penetration in the triaxial test,” Geotechnical Testing Journal, 7, 2, 70-76, 1984.
Yoshida N and Finn WDL. “Simulation of liquefaction beneath an impermeable surface layer,” Soil Dynamics and Earthquake Engineering, 19, 333-338, 2000.
Zienkiewicz OC and Shiomi T. “Dynamic behavior of saturated porous media: The generalized Biot formulation and its numerical solution,” International Journal for Numerical and Analytical Method in Geomechanics, 8, 71-96, 1984.